Special Issue Article

Journal of Molecular Recognition

Received: 18 July 2011, Revised: 11 January 2012, Accepted: 11 February 2012, Published online in Wiley Online Library

(wileyonlinelibrary.com) DOI: 10.1002/jmr. 2180

Modulation of imprinting efficiency in nanogels with catalytic activity in the Kemp elimination†

Paolo Bonomi, Ania Servant and Marina Resmini*

The interactions between the template and the functional monomer are a key to the formation of cavities in the imprinted nanogels with high molecular recognition properties. Nanogels with enzyme-like activity for the Kemp elimination have been synthesized using 4-vinylpyridine as the functional monomer and indole as the template. The weak hydrogen bond interaction in the complex is shown to be able to induce very distinctive features in the cavities of the imprinted nanogels. The percentage of initiator used in the polymerisation, ranging from 1% to 3%, although it does not have a substantial effect on the catalytic rate, reduces considerably the imprinting efficiency. The alteration of the template/monomer ratio is also investigated, and the data show that there is considerable loss of imprinting efficiency. In terms of substrate selectivity, a number of experiments have been performed using 5-Cl-benzisoxazole as substrate analogue, as well as 5-nitro-indole as template analogue for the preparation of a different set of nanogels. All the kinetic data demonstrate that the chemical structure of the template is key to the molecular recognition properties of the imprinted nanogels that are closely tailored and able to differentiate among small structural changes. Copyright © 2012 John Wiley & Sons, Ltd.

Keywords: imprinted polymers; enzyme mimic; kemp elimination; catalytic nanogels; enzyme-like catalysis; imprinting efficiency

INTRODUCTION

Enzymes are nature's tools that have evolved to maximize their ability to catalyse a chemical reaction with high efficiency (Kirby, 1996; Flavin and Resmini, 2009). There have been considerable efforts to develop systems able to mimic the activity of enzymes, not only to gain a better understanding of their mechanisms but also to prepare novel catalysts that can complement enzymes' vast repertoire (Meekel *et al*., 1996; Wulff, 2002). Molecular imprinting (Wulff and Sarhan, 1972; Carter and Rimmer, 2002), where a template is used in combination with monomers in a casting-type procedure to generate recognition sites, has been successfully used as a viable approach for the generation of polymers with enzyme-like activities (Wulff, 2002; Alexander *et al*., 2006). The application of this approach in recent years to microgels and nanogels, polymeric materials with a cross-linked but flexible matrix (Graham and Cameron, 1998), has increased the potential for applications (Markowitz *et al*., 2000; Ye and Mosbachm, 2001; Spegel *et al*., 2003; Fernandez-Barbero *et al*., 2009; Lyon *et al*., 2009). These materials have been shown to catalyse not only simple reactions, such as ester and carbonate hydrolysis (Maddock *et al*., 2004; Pasetto *et al*., 2005; Pasetto *et al*., 2009), but also more energetically challenging reactions such as the aldol condensation (Carboni *et al*., 2008). In all these cases, the key template–monomer interaction was based on strong ionic bonds or reversible co-valent interactions (Wulff *et al*., 1977; Liu and Wulff, 2004; Mayes and Whitcombe, 2005).

We recently reported the synthesis and characterisation of water-soluble imprinted nanogels with enzyme-like activity in the Kemp elimination reaction of 1,2-benzisoxazole, using indole as the template and 4-vinylpyridine (Ikeda *et al*., 1983; Yilmaz and Kucukyavuz, 1993) as the functional monomer, as shown in Scheme 1 (Servant *et al*., 2011). We were able to show that weak hydrogen bond interactions between the template and monomer,shown in Figure 1, can successfully lead to imprinted nanogels able to function as catalysts in water and that the addition of surfactant like Tween 20 has an effect on the catalytic activity as well as the morphology of the nanoparticles.

The Kemp elimination is the base-catalysed isomerization of 1,2-benzisoxazole (**1**) resulting in the formation of a single chromophoric product 2-cyanophenol (**3**), occurring via a single concerted one-step mechanism.

This reaction is not catalysed by enzymes, and a number of different approaches have been used to develop novel catalysts, such as synzimes, antibodies, and natural coils (Kemp *et al*., 1975). Our initial work focussed on the synthesis of nanogels, which were never used before for this reaction, and on the use of surfactants to enhance the catalytic activity. Despite the interesting results obtained thus far, further work is necessary to fully understand how molecular recognition and catalytic efficiency can be tuned for the required applications. There is a clear need to understand how the different parameters influence the morphology and characteristics of the nanogels and ultimately the catalytic changes in activity. It is important to underline that although considerable work has been carried

* *Correspondence to: M. Resmini, School of Biological and Chemical Sciences, Queen Mary University of London, Mile End Road, London E1 4NS, UK. E-mail: m.resmini@qmul.ac.uk*

† *This article is published in Journal of Molecular Recognition as part of the special issue on MIP2010: The Future of Molecular Imprinting, edited by David A. Spivak (Louisiana State University) and Kenneth J. Shea (University of California, Irvine).*

P. Bonomi, A. Servant, M. Resmini
School of Biological and Chemical Sciences, Queen Mary University of London, Mile end road, London E1 4NS, UK

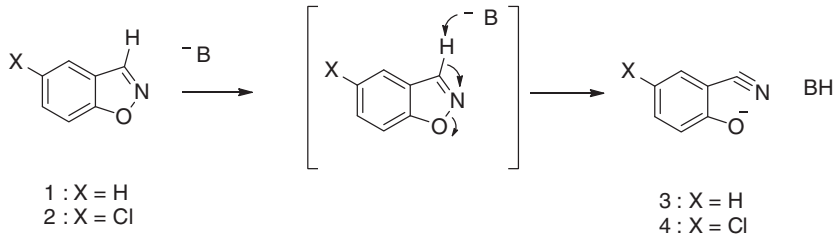

1 : X = H
2 : X = Cl

3 : X = H
4 : X = Cl

Scheme 1. Formation of products **3** and **4** from compounds **1** and **2** through the Kemp elimination reaction.

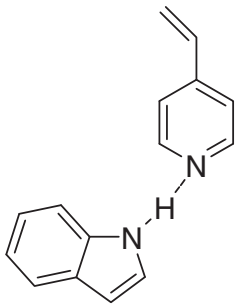

Figure 1. Hydrogen bond interaction between the template indole and the functional monomer 4-vinylpyridine.

out with imprinted polymers with binding properties (Spivak, 2005), the recognition characteristics and properties of catalytic imprinted polymers have yet to be fully studied and that the conclusions obtained in one field cannot be directly transferred to the other one.

In the present work, we report our results on the optimisation and in-depth characterisation of the catalytic activity of imprinted nanogels in the Kemp elimination. Our data indicate that the cross-linker concentration and the template/monomer ratio can influence the catalytic activity and the imprinting efficiency of the nanogels. The extensive and detailed kinetic studies using substrate analogues and template analogues with imprinted and non-imprinted nanogels demonstrate that even when using weak hydrogen bonds for the imprinting complex, the chemical structure of the template plays a key role in determining the recognition characteristics and the catalytic efficiency of the polymeric matrix.

EXPERIMENTAL SECTION

Chemicals and materials for substrate and nanogel synthesis

4-Vinylpyridine (%), ethylene glycol dimethacrylate (EGDMA, 98 %), indole (98%) and 5-nitroindole (98%), hydroxylamine hydrochloride (98%, ACS reagent) were purchased from Aldrich Chemical Co. (Gillingham, Dorset, UK). 4-Vinylpyridine and EGDMA were purified by vacuum distillation before use. 2,2′-Azobisisobutyronitrile (AIBN, 98%) was purchased from Acros Fisher Scientific UK (Loughbrough, Leicestershire) and recrystallized from methanol before use. 2-Hydroxy-5-nitrobenzaldehyde (97%) was purchased from Fluka (Gillingham, Dorset, UK). Anhydrous 1,2-dichloroethane (99%) was purchased from Aldrich Chemical Co. (Gillingham, Dorset, UK). Dialysis membranes were purchased from Medicell International Ltd, 3500/2 size, 22.0-mm diameter, molecular weight cut-off 3500 Da.

All the deuterated solvents for NMR studies were purchased from Cambridge Isotope Laboratories. Inc. Other solvents used for polymerizations or analytical experiments were of analytical grade. Sodium carbonate was purchased from BDS. 1,2-Benzisoxazole (98%) was purchased from Aldrich Chemical Co. (Gillingham, Dorset, UK).

Proton (^{1}H NMR) and carbon (^{13}C NMR) were recorded at 400 MHz on a Brucker Avance III 400 spectrometer. Chemical shifts (δ) are given in part per million (ppm), and coupling constants (*J*) are given in Hertz (Hz). UV–vis samples were analysed using a Varian Cary 300 BIO UV–vis spectrophotometer, equipped with an internal thermostat.

Interactions between templates (indole and 5-NO_2-indole) and *d5*-pyridine

Stock solutions of indole and 5-nitroindole were prepared in different deuterated solvent systems such as *d6*-dimethylsulfoxide (DMSO), *d3*-acetonitrile, CD_2Cl_2, $CDCl_3$, *d8*-toluene, and D_2O at a concentration of 85.4 mM. Spectra of indole in these different solvents were recorded. Increasing quantities of *d5*-pyridine from zero to seven equivalents were added to the indole solutions, and the spectra of indole and *d5*-pyridine at different equivalents were recorded. The chemical shift variation $\Delta\delta_H$ of the proton bound to the indole nitrogen was calculated and plotted against deuterated pyridine concentration. The data obtained could be fitted using Sigma plot 8 software into a hyperbola, and the binding constant was then determined using the ligand binding equation as follows:Determination of the binding constant by NMR titration:

$$\Delta\delta_H = \frac{A * x}{K_D + B * x}$$

where $\Delta\delta_H$ is the variation of chemical shift of the nitrogen proton of indole, *x* is the concentration of *d5*-pyridine, K_D is dissociation constant of the complex formation, and *A* and *B* are constants.

The same procedure as for indole was applied to 5-nitroindole.

Synthesis of the substrate 5-chloro-benzisoxazole

Synthesis of 5-Cl-salicylaldoxime

Aqueous sodium acetate (1.2 ml, 5.75 × 10^{-3} mol, 1.9 eq.) was added to a warm solution of 5-chlorosalicyladehyde (472 mg, 3.05 × 10^{-3} mol, 1.0 eq.) and hydroxylamine hydrochloride (418 mg, 6.1 × 10^{-3} mol, 2.0 eq.) to a solution of acetonitrile/water (60% acetonitrile, 6 ml). The clear solution was heated at reflux for 3 hr. The clear orange solution was cooled down to room temperature, and 3 ml of water was added to the mixture. The solution was then kept at 4 °C in an ice bath. The formation of light yellow needles was observed. The solid was filtered off, washed with water, and then freeze dried. The yield was 76.4%.

^{1}H-NMR (400 MHz, $CDCl_3$): δ 6.93 (d, J = 8.8 Hz, 1H), 7.16 (d, J = 2.3, 1H), 7.25 (dd, J_1 = 8.8 Hz, J_2 = 2.3 Hz, 1H), 7.6 (br, 1H), 8.16 (s, 1H), 9.75 (br, 1H)

Synthesis of 5-chlorobenzisoxazole

The oxime (410 mg, 2 mmol) was dissolved in anhydrous tetrahydrofurane (THF) (5 ml), and 2 ml of a solution of trichloroacetyl isocyanate in THF (2 M, 4 mmol) was added under anhydrous conditions. The solution was stirred for 10 min before anhydrous potassium carbonate (286 mg, 2.7 mmol) was added. The mixture was stirred for 30 min before adding 7 ml of 0.1 M HCl. The solution was stirred for an additional 10 min. THF was then evaporated, and the aqueous phase was extracted with dichloromethane. The combined organic phases were dried with magnesium sulphate. After evaporation of the dichlormethane, a light yellow solid was recovered. The compound was recrystallized twice with acetonitrile and water. A mass of 163.2 mg of the product as a white solid was recovered. The yield was 44%.

^{1}H-NMR (400 MHz, $CDCl_3$): δ 7.53 (dd, J_1 = 8.9 Hz, J_2 = 1.8 Hz, 1H), 7.57(d, J = 8.9 Hz, 1H), 7.72 (d, J_1 = 1.8, 1H), 8.68 (s, 1H).

Synthesis of the 5-chloro-2-cyanophenol

A solution of 5-chlorobenzisoxazole (0.3 g, 1.95 mmol) in 5 ml of acetonitrile and 5 ml of water was mixed with 15 ml of a solution of 3 M NaOH and was allowed to stir for 10 min. Concentrated HCl was added drop-wise to the latter solution to bring down the pH to 1. The solution was extracted three times with 10-ml portions of dichloromethane, and the extracts were combined and dried over magnesium sulphate. The solvent was evaporated, and the solid residue was recrystallized with acetonitrile. The recrystallized solid was dried under vacuum overnight and stored in foil-wrapped vials in the freezer. A UV–vis spectrum was recorded to test the purity of the compound. Maximum absorbance was recorded at a wavelength of 339 nm in agreement with the literature.

UV–vis: λ_{max} in acetonitrile: 339 nm; ^{1}H-NMR (400 MHz, acetonitrile (ACN)-*d*3): δ 6.98(dd, J_1 = 8.9, 1H), 7.44 (dd, J_1 = 10 Hz, J_2 = 2.6 Hz, 1H), 7.56 (d, J_1 = 2.6, 1H), 7.9 (br, 1H).

Titration of nanogels for the determination of pyridine residues

A 20-ml solution of imprinted nanogels was prepared at a concentration of 1 mg ml^{-1} in 20% acetonitrile in distilled water. To the latter was added 15 ml of HCl solution at a concentration of 4×10^{-3} M. The mixture was then allowed to stir for a few minutes, and the pH of the solution was recorded. The resulting nanogel solution was titrated using a NaOH solution at a concentration of 1.5×10^{-3} M. The pH was recorded every milliliter and half milliliter around the equivalent points area, and the values were plotted against the volume of NaOH solution. The equivalent points were determined manually, and the volume at the equivalence was determined as the mean from the three measurements. The exact same procedure was applied to the non-imprinted nanogel. The concentration of pyridine moieties C_{Py} was determined by the volume difference between the two equivalent points and the knowledge of the titrant (NaOH) concentration C_{NaOH} as explained in the following equation:

$$C_{Py} = \frac{(V_{e2} - V_{e1}) \times C_{NaOH}}{V}$$

where V_{e1} and V_{e2} are the volume at the first and second equivalent point, respectively, and V is the volume of the polymer solution before titration.

RESULTS AND DISCUSSION

Our previous work demonstrated that the choice of pH and the percentage of organic solvent in the reaction solutions, together with the addition of surfactants (Ashbaugh *et al*., 2000; Barreiro-Iglesias *et al*., 2001; Barreiro-Iglesias *et al*., 2003), had a direct impact on the imprinting efficiency of the catalytic nanogels, defined as the ratio between the rate constants for the imprinted nanogels and those for the non-imprinted nanogels, and on the morphology of the nanoparticles (Servant *et al*., 2011). This prompted further studies aiming to investigate the influence of polymerisation parameters such as initiator content and functional monomer/template ratio on the properties of the nanogels. It was expected that these parameters would have a direct effect on the polymer morphology and on the concentration of active site (Resmini *et al*., 2000) and therefore would alter the catalytic activity of the nanoparticles. There is very little knowledge and detailed information on how the efficiency and molecular recognition properties of these materials can be modulated to obtain novel catalysts with enzyme-like activities.

Study of the effect of initiator content

The first part of the work focussed on the evaluation of the effect of changing the concentration of initiator in the polymerisation reaction. The nanogels were prepared using high-dilution polymerisation using AIBN as initiator, following an established protocol (Maddock *et al*., 2004) and the experimental conditions that had been previously shown to be optimal, that is, total monomer concentration C_M 0.5% in mass and 80% of EGDMA as cross-linker in DMSO (Maddock *et al*., 2004). In each case, two nanogels preparations were synthesized, both containing the functional monomer 4-vinylpyridine, one imprinted (MIP) and one non-imprinted (NIP). Three sets of polymers were prepared with initiator content equal to 1%, 2%, and 3% of the quantity of double bonds in the pre-polymerisation mixture. To obtain meaningful comparison of kinetic data for the polymer preparations, it was necessary to estimate the concentration of functional groups available. This was done by back-titration of the pyridinium ions using NaOH. The titration curves for MIP AS232 and MIP AS234 are shown in Figure 2. Similar curves were obtained for MIP AS230, NIP AS231, NIP AS233, and NIP AS235.

The concentration of pyridine moieties available in the nanogels was obtained from the difference in NaOH volume required to reach the two different equivalence points. The data, in Table 1, regarding active site concentrations, show that in each of the three sets, there is no significant difference between the imprinted and non-imprinted nanogels, which indicates that the presence of the template does not have an effect on the polymerisation process and in the rate of incorporation of the functional monomer 4-vinylpyridine. When comparing all six nanogels, it appears that although the preparations with 1% and 2% initiator show similar results, the one with 3% appears to have a higher incorporation of functional monomer. These data have been consistently obtained in repeat experiments and can be possibly explained by the overall higher rate of polymerisation due to the higher initiation content.

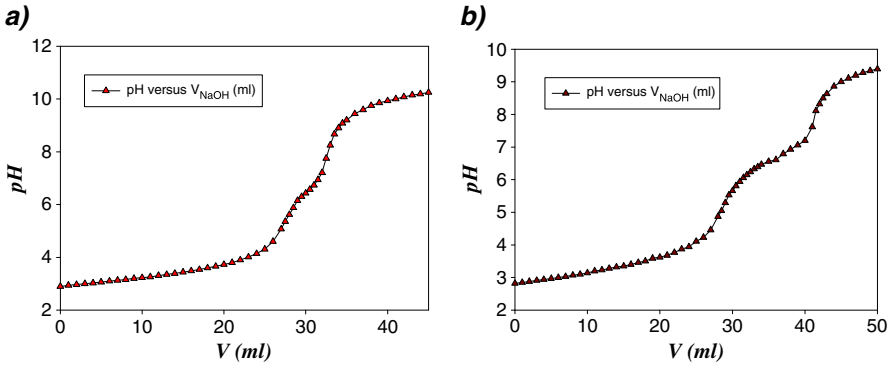

Figure 2. Titration curves of (a) MIP AS232 and (b) MIP AS234 using a solution of NaOH at a concentration of 1.5×10^{-3} M.

These polymers were then used to carry out kinetic experiments using 1,2-benzisoxazole (**1**) as the substrate, at pH 9.4 (0.05 M carbonate buffer) with 10% ACN and 1 mg/ml of nanogels, and monitoring product formation at $\lambda = 325$ nm using UV–vis spectroscopy. Initial rates (v_i) for both imprinted and non-imprinted nanogels were obtained and corrected for the uncatalysed rate and divided by the active site concentration to give the apparent rate constant (k'_{app}) that was used to obtain some qualitative indication of trends.

The kinetic data showed that the initiator content appeared to have a noticeable effect on the catalytic properties of the nanogels. An initial analysis showed that NIP AS233, MIP AS234, and NIP AS235 did not display a saturation curve in the range of substrate concentrations investigated; it was therefore not possible to determine kinetic parameters such as the rate constant k_{cat} and catalytic efficiency k_{cat}/K_M. This was most likely due to higher values of K_m for the non-imprinted polymers, outside the range of the substrate concentration being evaluated.

To compare the nanogels with different AIBN content, the values of apparent rate constant k'_{app} and the apparent imprinting factor were calculated for a single-substrate concentration (2 mM), and the values are gathered in Table 1. This substrate concentration was selected because at this value a significant difference between imprinted and non-imprinted polymers was observed and a saturation curve was obtained for MIP AS230 and MIP AS232. The data clearly show that as the concentration of initiator is increased from 1% to 3%, the catalytic efficiency of the nanogels decreases, and, more significantly, the imprinting efficiency is also reduced, and in the case of the 3% initiator, there is no relevant difference between the imprinted and non-imprinted nanogels. This would suggest that although higher initiator content results in higher incorporation of functional monomer, especially with 3%, the apparent imprinting efficiency, measured at a single substrate concentration, is lowered.

Evaluation of the effect of the template/monomer ratio on the catalytic efficiency

In an effort to further optimize the preparation of the imprinted nanogels with enhanced activity and imprinting efficiency, it was decided to alter the ratio template/monomer and to study the effect on the catalytic activity and on the imprinting efficiency to evaluate whether there was any significant effect. The idea was that the change in the template/monomer ratio could favour the association of these two molecules toward complex formation, therefore creating more specific cavities. This was done by synthesising the nanogels using an excess of template in the first instance and then an excess of functional monomer and evaluating the results.

Two sets of imprinted and non-imprinted nanogels (MIP AS250/NIP AS251 and MIP AS252/NIP AS253) were prepared, under identical conditions, with two and five equivalents of indole compared with 4-vinylpyridine, respectively, and the catalytic activities were compared with the preparations MIP AS230 and NIP AS231, which were prepared with a 1:1 ratio of template and functional monomer. As previously, the number of active sites was determined via back-titration and used to calculate the kinetic parameters.

The data regarding the active site concentration, shown in Table 2 for all six nanogel preparations, are all in a very similar order of magnitude. Therefore, the addition of a large excess of template does not appear to have a substantial effect in the incorporation of 4-vinylpyridine.

The kinetic experiments, carried out at 2 mM substrate concentration, show that the nanogels prepared with 1:1 template/monomer ratio have the highest catalytic activity, as indicated by the value of the apparent rate constant. The excess of indole was expected to favour the template–monomer equilibrium toward the complex formation, increasing the amount of specific cavities formed during the imprinting process. This does not appear to be the case. The polymers MIP AS250 and MIP AS252 did not show any significant change in imprinting efficiency compared with the

Table 1. Kinetics parameters for MIP AS230, AS232, AS234 and NIP AS231, AS233, and AS235 (at pH 9.4, 10% ACN, 1 mg/ml of nanogels)

Polymers	AIBN content	v_i (μM min^{-1})	Active site (μmol mg^{-1})	k'_{app} (min^{-1})	$k'_{app,MIP}/k'_{app,NIP}$
MIP AS230	1	0.61	0.24	2.54	1.61
NIP AS231	1	0.30	0.19	1.58	—
MIP AS232	2	0.49	0.28	1.75	1.23
NIP AS233	2	0.37	0.26	1.42	—
MIP AS234	3	0.70	0.52	1.34	1.1
NIP AS235	3	0.73	0.60	1.22	—

Table 2. Kinetics parameters for MIP AS230, MIP AS250, MIP AS252 and NIP AS231, NIP AS251, and NIP AS253 (pH 9.4, 10% ACN, 1 mg/ml nanogels)

Polymers	Template equivalents	v_i (μM min^{-1})	Active site (μmol mg^{-1})	k'_{app} (min^{-1})	$k'_{app,MIP}/k'_{app,NIP}$
MIP AS230	1	0.61	0.24	2.54	1.6
NIP AS231	1	0.30	0.19	1.58	—
MIP AS250	2	0.42	0.58	0.72	1.4
NIP AS251	2	0.23	0.45	0.51	—
MIP AS252	5	0.48	0.38	1.26	1.5
NIP AS253	5	0.38	0.45	0.84	—

one exhibited by MIP AS230 (nanogels synthesized with one equivalent of template).

Work on the evaluation of template effect on the selectivity of imprinted polymers was reported in previous studies by Mosbach *et al*. for the generation of binding "bulk" nicotine-imprinted polymers (Andersson *et al*., 1999). In this work, it was demonstrated that an excess of template during the polymerisation process was clearly unfavourable with regard to selectivity, leading to the generation of cavities with high heterogeneity, poor binding activity, and low imprinting efficiency. Other groups have also investigated and reviewed this issue in the context of binding polymers (Manesiotis *et al*., 2004; Sellergren and Allender, 2005; Spivak, 2005; Yoshimatsu *et al*., 2011).

The highest catalytic activity obtained in our case with a 1:1 ratio would indicate that the excess of template does not favour an increased selectivity and specificity in the catalytic polymers; however, the imprinting efficiency as determined by the ratio of the apparent catalytic constants is not affected, and this could be the result of using catalytic parameters to evaluate the imprinting effect, which differs completely for how it is done with binding polymers.

In the second approach, the effect of using an excess of functional monomer on the kinetic parameters was studied. One set of nanogels was prepared using seven equivalents of 4-vinylpyridine and C_M of 0.5% and 80% of EGDMA as cross-linker, and MIP AS242 and NIP AS243 were synthesized using the standard protocol of high-dilution radical polymerisation.

Active site titration for the nanogels was carried out, and the results showed that although these polymers contained 15% more pyridine units compared with MIP AS230 and NIP AS231, this did not correlate significantly with the much higher amount of functional monomer used in the preparation, indicating a very low incorporation. Analysis of the kinetic data shows that although both nanogel preparations, MIP AS242 and NIP AS243, demonstrated catalytic activity in the Kemp elimination when compared with the background reaction (k_{uncat} was found to be $8.18 \times 10^{-4} \pm 1.03 \times 10^{-21}$ min^{-1}), the data could not be fitted to a Michaelis–Menten saturation curve but only to a linear regression. In addition, there was no significant difference between the reaction rates for the imprinted and non-imprinted nanogels. This suggests that although the percentage of functional monomer incorporated is only marginally increased, the imprinting efficiency evaluated using the kinetic parameters has changed dramatically. The fact that the kinetic data could not be fitted with a saturation curve is a clear indication that the substrate range evaluated was well below the value of K_M. This indicates a much lower binding affinity between the cavity and substrate, therefore leading to a possible explanation being that the higher amount of monomer used has got a significant effect on the polymerisation process leading to a loss of imprinting efficiency. A similar effect, although related to binding polymers, was also reported by Andersson *et al*. in the preparation of binding "bulk" nicotine-imprinted polymers (Andersson *et al*., 1999), where an excess of methacrylic acid led to a decrease of the selectivity of the polymers.

Molecular recognition and substrate selectivity

Having evaluated the effect of important polymerisation parameters, such as initiator content and template/monomer ratios, on the activity of the nanogels, the next step focussed on the study of the molecular recognition properties in relation to catalysis. An important criterion in the development of enzyme mimics is the ability of these tailor-made catalysts to specifically recognize a substrate molecule and, in a similar way as enzymes, to form a complex and generate the product of the targeted reaction. One of the advantageous features of the molecular imprinting approach is the possibility of forming a tailored site complementary to a target molecule into a polymeric network, which allows the specific recognition of this molecule similarly to the "lock-and-key" system (Li *et al*., 2008). Some early work in the field was carried out by Shea's group, where imprinted polymers with esterolytic activity were shown to have a degree of stereoselectivity, as a result of hydrogen bonding in the binding step (Sellergren and Shea, 1994). The work presented here was focussed on two different yet complementary strategies. In the first instance, the MIP AS230 and NIP AS231, imprinted with indole and non-imprinted, were evaluated as catalysts for the Kemp elimination using a substrate analogue, 5-Cl-benzisoxazole (**2**), a molecule that differs from the cognate substrate benzisoxazole for the presence of the chlorine atom in the *para* position. In the second instance, new nanogels were synthesized, using 5-nitroindole as the template analogue, and the catalytic activity toward 1,2-benzisoxazole (**1**) and 5-chloro benzisoxazole (**2**) was evaluated and compared.

The structures of 5-nitroindole and 5-chlorobenzisoxazole are shown in Figure 3.

The choice of using 5-Cl-benzisoxazole (**2**) as substrate analogue, with an electron-withdrawing group like the chlorine atom in *para* to the oxygen atom, was expected to enhance the rate of the

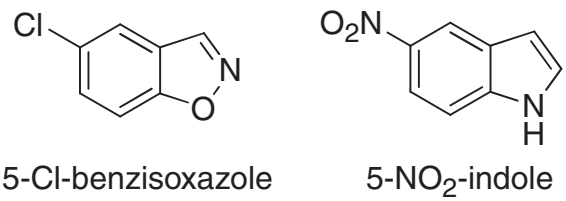

Figure 3. Structure of 5-Cl-benzisoxazole and 5-NO_2-indole.

Journal of Molecular Recognition

reaction due to the change in electron environment and distribution (Casey *et al.*, 1973). The removal of the proton is more favoured in the presence of electron-withdrawing groups in that position.

To have accurate kinetic data, calibration curves for both products were obtained to give extinction coefficient values: The value of ε for 5-Cl-cyanophenol (**4**) was found to be 56140 cm^{-1} M^{-1}, whereas for 2-cyanophenol (**3**), the extinction coefficient (ε) was 5940 cm^{-1} M^{-1}. The reactions were all carried out under the same experimental conditions (carbonate buffer 50 mM pH 9.4 with a 10% of acetonitrile and 0.5% of Tween 20), and experiments were carried out with both substrates in the absence of any nanogels to evaluate the uncatalysed reaction rates.

The k_{uncat} for 1,2-benzisoxazole (**1**) was found to be 4.30×10^{-4} (SE $\pm$ 5.20×10^{-5}), whereas in the case of 5-Cl-benzisoxazole (**2**), the k_{uncat} registered was 9.80×10^{-4} (SE $\pm$ 2×10^{-4}) showing the expected increase as a result of the substituent. All reactions were carried out using a fixed concentration of nanogels (0.02 mg ml^{-1}), whereas substrate concentration varied between 0.2 mM and 1.2 mM. Initial rates were determined by monitoring product formation at 339 nm for 5-Cl-2-cyanophenol (**4**) and 325 nm for 2-cyanophenol (**3**) and were all corrected for the uncatalysed reaction.

Because MIP AS230 and NIP AS231 displayed a saturation curve in the range of the substrate concentration investigated, it was possible to fit the data using the hyperbola equation, in agreement with the Michaelis–Menten model (Figure 4).

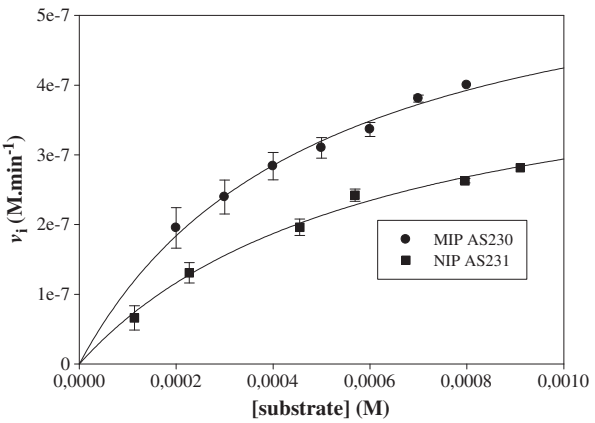

Figure 4. Initial rates versus substrate concentration plots for MIP AS230 and NIP AS231 on 5-Cl-benzisoxazole ([nanogel] = 0.02 mg ml^{-1}, pH 9.4, 50 mM carbonate buffer, 10% ACN, 0.5% Tween 20). All initial rates are corrected for the uncatalysed reaction.

The experimental data for the activity of both polymers toward substrate **2**, shown in Figure 4, were used to obtain the kinetic parameters, and these were found to be V_{max} 6.30×10^{-7} (SE $\pm$ 4.0×10^{-8}) M min^{-1}, K_M 4.87×10^{-4} (SE $\pm$ 6.50×10^{-5}) M, for MIP AS230. For NIP AS231, the values obtained were V_{max} of 4.75×10^{-7} (SE $\pm$ 4.04×10^{-8}) M min^{-1} and K_M of 6.16×10^{-4} (SE $\pm$ 1.50×10^{-4}) M, also reported in Table 3. The first interesting observation is that when the concentration of active sites is taken into account, comparison of the values of the catalytic rate constant shows that the imprinted nanogel AS230 has higher activity and displays a catalytic efficiency equal to 2, despite the substrate analogue **2** having both steric and electronic differences compared with the cognate substrate **1**. The values of the K_M unfortunately carry a significant standard deviation value ranging between 13% and 25%, as a result of not being able to increase the substrate concentration high enough, therefore limiting any possible discussion. This is an interesting result that indicates that the imprinting approach, even when using weak hydrogen bonding, is certainly sensitive to the microenvironment and that the molecular recognition properties induced in the active sites are specific and dependent on the structure of the template used.

When the kinetic data for substrate **2** are compared with the ones for 1,2-benzisoxazole (**1**), also reported in Table 3, it becomes apparent that (i) the imprinted nanogels MIP AS230 are catalytically more efficient when working on the cognate substrate, as indicated by the higher value of k_{cat}, and (ii) more significantly, the imprinting factor when using the cognate substrate **1** is two times higher than with the substrate analogue **2**.

The cavities in the MIPs are specifically tailored for the template used in the polymerization process, and for this reason, AS230 is showing a higher affinity for a molecule, like substrate **1**, that is a very close mimic, from a structural and chemical point of view, of the indole template. The variation in the catalytic efficiency can be explained by a combination of electronic and steric differences between the chemical structures of substrate **2** and the indole template.

Having evaluated the specificity and molecular recognition properties, coupled with specific catalytic activities, of the indole-imprinted polymers, it was decided to investigate further the selectivity by preparing new nanogels imprinted with a different template. 5-Nitrobenzisoxazole was selected as the template, as the molecule contains the nitro functional group, which increases the steric hindrance of the template and also provides important changes in the electronic effect of the

Table 3. Active site concentrations and kinetics parameters for MIP(s) AS230, AS238 and NIP(s) AS231, AS239 reacting with cognate substrate **1** and analogue **2**

Catalyst	Substrate	V_{max} (μM min^{-1})	K_M (M)	k_{cat} (min^{-1})	Active site in the reaction (μM)	k_{catMIP}/k_{catNIP}
AS230	2	0.63	4.87×10^{-4}	1.13	0.56	2
AS231	2	0.47	6.16×10^{-4}	0.56	0.84	—
AS230	1	1.54	1.58×10^{-3}	2.75	0.56	3.4
AS231	1	0.69	1.83×10^{-3}	0.82	0.84	
AS238	2	0.53	4.17×10^{-4}	1.33	0.40	1.8
AS239	2	0.26	7.60×10^{-4}	0.72	0.36	—
AS238	1	0.90	1.00×10^{-3}	2.25	0.40	4
AS239	1	0.20	5.36×10^{-4}	0.56	0.36	—

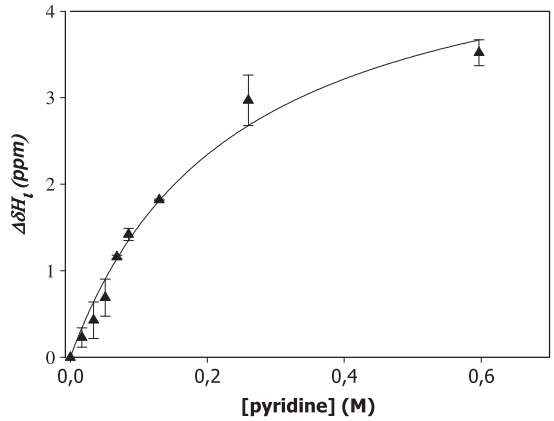

Figure 5. Plot of the variation of chemical shifts $\Delta\delta_H$ of the proton bonded to the N of the template, corrected from the value of the chemical shift of H_i of 5-nitroindole alone versus the concentration of d_5-pyridine.

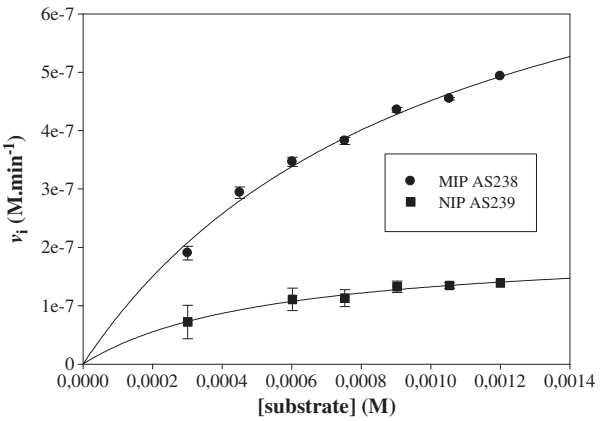

Figure 6. Plot of initial rates versus substrate concentration for nanogels MIP AS238 and NIP AS 239 on 1,2 benzisoxazole (**1**) ([nanogel] = 0.02 mg ml^{-1}, pH 9.4, 50 mM carbonate buffer, 10% ACN, 0.5% Tween 20). All initial rates are corrected for the uncatalysed reaction.

molecule. In addition, given the high polar nature of the group, there is also the possibility that additional interaction points may arise as a result of hydrogen bonding between the template and the monomers/cross-linker. The pK_a of the nitrogen proton of 5-nitroindole is found to be around 14.75, a value very close to that one of indole (pK_a 16). The presence of the strong electron-withdrawing and sterically bulky substituent was expected to provide significant effects to the catalytic activity and molecular recognition properties of the nanogels.

It was not possible to evaluate the catalytic activity of these new nanogels with the corresponding cognate substrate 5-nitro-benzisoxazole due to the need to work at a much lower pH to be able to carry out kinetic studies. There was clear concern that this could impact the morphology of the nanogels, therefore preventing any comparison to be 121carried out. Instead, it was decided to test the activity on two substrate analogues to evaluate any differences in molecular recognition.

The first step, toward the synthesis of the nanogels, was to study the interaction between 5-nitroindole and the functional monomer 4-vinylpyridine. A non-covalent hydrogen bonding between the proton on the nitrogen of the indole derivative and the lone pair of the nitrogen of 4-vinylpyridine was expected to be similar to that one exhibited in the case of the non-substituted indole. The interaction studies were carried out in a similar way using ^{1}H-NMR spectroscopy, studying the variation of chemical shift of the proton on the nitrogen atom of the template (Wilcox *et al*., 1992).

A solution of 5-nitroindole was prepared at a concentration of 85.4 mM in CD_2Cl_2, and increasing equivalents of *d5*-pyridine ranging from 0.2 (1.7×10^{-2} M) to 7 equivalents (5.9×10^{-1} M) were added to the solution. The spectra of indole alone and for each equivalents of pyridine were recorded. The values of δ_H were collected and plotted against the concentration of *d5*-pyridine, as shown in Figure 5.

A variation of the chemical shift of the proton from δ 8.76 to δ 12.3 was noticed, which confirmed the interaction via non-covalent hydrogen bond between 5-nitroindole and 4-vinylpyridine. The association constant K_{ass} was found to be around 0.42 M^{-1}. The interactions between 5-nitroindole and pyridine appeared to be stronger than in the case of indole, and this is clearly the result of the presence of the

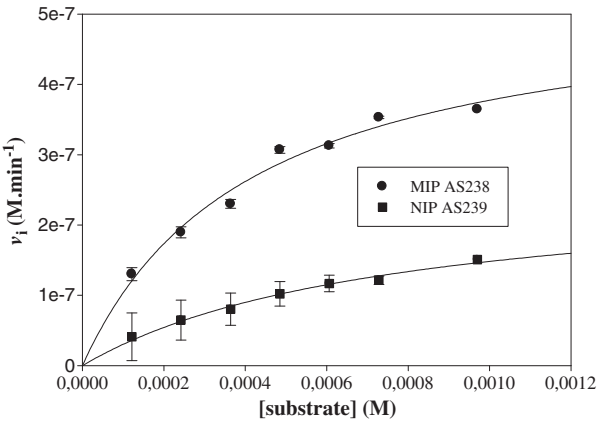

Figure 7. Plots of intial rates versus substrate concentration for MIP AS238 and NIP AS239 on 5-Cl-benzisoxazole (**2**) ([nanogel] = 0.02 mg ml^{-1}, pH 9.4, 50 mM carbonate buffer, 10% ACN, 0.5% Tween 20). All initial rates are corrected for the uncatalysed reaction.

substituent. A set of imprinted and non-imprinted nanogels, MIP AS238 and NIP AS239, were prepared with 5-nitroindole as template molecule, using the standard protocol of high-dilution radical polymerisation (Graham and Cameron, 1998). The determination of the active site number was performed using the standard procedure of back-titration of pyridine residues described in the experimental session. The active site number obtained for MIP AS238 was found to be 0.20×10^{-6} µmol mg^{-1} and 0.18×10^{-6} µmol mg^{-1}. These values were found to be within the range of active site concentrations obtained with previous polymers preparations.

A detailed kinetic study of the catalytic activity of MIP AS238 and NIP AS239 with both substrates 5-chlorobenzisoxazole (**2**) and 1,2-benzisoxazole (**1**) was carried out. All the reactions were performed under the same conditions previously described, using 0.02 mg ml^{-1} of nanogels in 50 mM carbonate buffer, pH 9.4, 10% ACN, and 0.5% Tween 20. The initial rates, corrected for the background reactions, were plotted versus substrate concentration as shown in Figure 6.

Both nanogels MIP AS238 and NIP AS239 demonstrated catalytic activity for the reaction toward the substrates, and, in all

cases, the data could be fitted into a Michaelis–Menten saturation curve to provide the kinetic parameters.

In particular, for MIP AS238 tested on 1,2-benzisoxazole (**1**), we obtained the following values: $V_{max} = 9.06 \times 10^{-7}$ (SE $\pm$ 7.034 $\times$ 10^{-8}) M min^{-1}, $K_M = 1.00 \times 10^{-3}$ (SE $\pm$ 1.424 $\times$ 10^{-4}) M, $k_{cat} = 2.25\,min^{-1}$. For NIP AS239, the values obtained were as follows: $V_{max} = 2.03 \times 10^{-7}$ (SE $\pm$ 1.25 $\times$ 10^{-8}) M min^{-1}, $K_M = 5.36 \times 10^{-4}$ (SE $\pm$ 7.98 $\times$ 10^{-5}) M, $k_{cat} = 0.56\,min^{-1}$.

These data indicate that MIP AS238 is a better catalyst than NIP AS239 due to the higher values of V_{max} and k_{cat}, but, if compared with the data obtained using the indole-imprinted polymer AS230, the catalytic activity of the indole-imprinted nanogels is still higher. Given that substrate **1** is sterically less hindered than the 5-nitroindole, it is still able to access the imprinted cavities of MIP AS238, and the smaller size may explain the smaller value of K_M compared with AS230.

The imprinting efficiency of the two sets of polymers, when evaluated against substrate **1**, is fairly similar. It is important to note that in this case, the kinetic characterisation was carried out using a full set of data, instead of a single-substrate concentration, and therefore, the imprinting efficiency is determined by the ratio of the values of catalytic constants for the MIP and NIP.

To compare the selectivity of these new catalysts (MIP AS238 and NIP AS239) with the indole-imprinted nanogels (MIP AS230 and NIP AS231) and to better investigate the effect of the size of the substrate on the affinity of the catalysts, we tested the 5-nitroindole-imprinted nanogels in the Kemp elimination using another substrate analogue, 5-Cl-benzisoxazole, a molecule that has a large substituent in the same position as in the template and is also electron-withdrawing.

A set of reactions were carried out using the same conditions reported before: carbonate buffer 50 mM, pH 9.4 with a 10% of acetonitrile and 0.5% of Tween 20, fixed concentration of the catalysts (0.02 mg ml^{-1}), and varying the concentration of 5-Cl-benzisoxazole (**2**) between 0.2 and 1 mM. The kinetic data, shown in Figure 7, were fitted to the hyperbola equation in agreement with the Michaelis–Menten model, and the kinetic parameters were found to be $V_{max} = 5.35 \times 10^{-7}$ (SE $\pm$ 4.25 $\times$ 10^{-8}) M min^{-1}, $K_M = 4.17 \times 10^{-4}$ (SE $\pm$ 7.65 $\times$ 10^{-5}) M, $k_{cat} = 1.34\,min^{-1}$. For NIP AS239, the values obtained were $V_{max} = 2.61 \times 10^{-7}$ (SE $\pm$ 2.47 $\times$ 10^{-8}) M min^{-1}, $K_M = 7.60 \times 10^{-4}$ (SE $\pm$ 1.3 $\times$ 10^{-4}) M, and $k_{cat} = 0.725\,min^{-1}$.

As demonstrated by the kinetic parameters, MIP AS238 is a superior catalyst than NIP AS239 showing higher k_{cat} whilst having a lower K_M. In this case, the standard deviation errors associated with the calculations of K_M are smaller than the difference between the two estimated values and therefore can be considered as real. This provides once more evidence that although the nanogels were imprinted with a different template, the imprinted and non-imprinted cavities show different kinetic behaviour toward the substrate analogue.

The interesting finding is related to the fact that when the activities of the 5-nitroindole-imprinted nanogels for the two different substrate analogues are compared, the data indicate that the 1,2-benzisoxazole is a better substrate, giving rise to higher catalysis and imprinting efficiency. The affinity of the 5-nitroindole-shaped cavities of MIP AS238 for a smaller molecule as 1,2-benzisoxazole is higher than in the case of a bigger compound as 5-Cl-benzisoxazole; once again, the size of the molecule seems to play an important role on the diffusion of the substrate into the three-dimensional active sites of the nanogels.

CONCLUSION

The potential of the molecular imprinting approach for the development of novel catalysts with enzyme-like activity is yet to be achieved. Although very significant results have been obtained thus far, these have frequently relied on very strong template–monomer interactions, which prove to be limiting in terms of wider applicability. The use of the more flexible nanogel matrix coupled with a better understanding of the factors that contribute to the molecular recognition properties of the cavities promises important advances. We have showed that it is possible to develop imprinted nanogel catalysts using weak hydrogen bond interactions, and in this work, we have presented a very detailed investigation of the effects of the different polymerisation parameters on the molecular recognition characteristics and on the imprinting efficiency. The data demonstrate that the chemical structure of the template plays a key role in determining the binding and catalytic properties of the cavities, which are then able to differentiate between minor structural differences in the substrates. The fine-tuning of the molecular recognition characteristics of the imprinted cavities together with the strategic design of the template and the functional monomer will provide new opportunities for novel catalysts.

Acknowledgements

The authors acknowledge the financial support of the European Commission via the Marie Curie actions (MCRTN-2006-033873 and MCIAPP-2009-251307) and Queen Mary University of London.

REFERENCES

Alexander C, Andersson HS, Andersson LI, Ansell RJ, Kirsch N, Nicholls IA, O'Mahony J, Whitcombe MJ. 2006. Molecular imprinting science and technology: a survey of the literature for the years up to and including 2003. *J. Mol. Recognit.* **19**: 106–180.

Andersson HS, Karlsson JG, Piletsky SA, Koch-Schmidt AC, Mosbach K, Nicholls IA. 1999. Study of the nature of recognition in molecularly imprinted polymers, II [1]: Influence of monomer–template ratio and sample load on retention and selectivity. *J. Chromatogr. A* **848**: 39–49.

Ashbaugh HS, Piculell L, Lindman B. 2000. Interactions of cationic/non-ionic surfactant mixtures with an anionic hydrogel: Absorption equilibrium and thermodynamic modeling. *Langmuir* **16**: 2529–2538.

Barreiro-Iglesias R, Alvarez-Lorenzo C, Concheiro A. 2001. Incorporation of small quantities of surfactants as a way to improve the rheological and diffusional behavior of carbopol gels. *J. Control. Release* **77**: 59–75.

Barreiro-Iglesias R, Alvarez-Lorenzo C, Concheiro A. 2003. Poly(acrylic acid) microgels (carbopol $^{(R)}$ 934)/surfactant interactions in aqueous media Part II: Ionic surfactants. *Int. J. Pharm.* **258**: 179–191.

Carboni DK, Flavin K, Servant A, Gouverneur V, Resmini M. 2008. The First Example of Molecularly Imprinted Nanogels with Aldolase Type I Activity. *Chem. Eur. J.* **14**: 7059–7065.

Carter SR, Rimmer S. 2002. Fabrication of High-Density, High Aspect Ratio, Large-Area Bismuth Telluride Nanowire Arrays by Electrodeposition into Porous Anodic Alumina Templates. *Adv. Mater.* **14**: 667–670.

Casey ML, Kemp DS, Paul KG, Cox DD. 1973. The physical Organic Chemistry of Benzisoxazoles. I. The Mechanism of the Base-Catalyzed Decomposition of Benzisoxazoles. *J. Org. Chem.* **38**: 2294–2301.

Fernandez-Barbero A, Suarez IJ, Sierra-Martin B, Fernandez-Nieves A, de Las Nieves FJ, Marquez M, Rubio-Retama J, Lopez-Cabarcos E. 2009. Gels and microgels for nanotechnological applications. *Adv. Colloid Interface Sci.* **147**: 88–108.

Flavin K, Resmini M. 2009. Imprinted nanomaterials: a new class of synthetic receptors. *Anal. Bioanal. Chem.* **393**(2): 437–444.

Graham NB, Cameron A. 1998. Nanogels and microgels: The new polymeric materials playground. *Pure Appl. Chem.* **70**: 1271–1275.

Ikeda N, Miyasaka H, Okada T, Mataga N.1983. Picosecond laser photolysis studies of deactivation processes of excited hydrogen bonding complexes. 3. Detection of the non fluorescent charge-transfer state in the excited 1-aminopyrene-pyridine hydrogen bonded pair and related systems. *J. Am. Chem. Soc.* **105**: 5206–5211.

Kemp DS, Paul KG. 1975. Physical Organic-Chemistry Of Benzisoxazoles. III. Mechanism And Effects Of Solvents On Rates Of Decarboxylation Of Benzisoxazole-3-Carboxylic Acids. *J. Am. Chem. Soc.* **97**: 7305–7312.

Kirby AJ. 1996. Enzyme Mechanism, Models and Mimics. *Angew. Chem. Int. Ed.* **35**: 706–724.

Li S, Huang X, Zheng M, Li W. 2008. Molecular imprinted polymers: modulating molecular recognition by a thermal phase transition in the binding framework. *Anal. Bioanal. Chem.* **392**: 177–185.

Liu JQ, Wulff G. 2004. Functional Mimicry of the Active Site of Carboxypeptidase A by a Molecular Imprinting Strategy: Cooperativity of an Amidinium and a Copper Ion in a Transition-State Imprinted Cavity Giving Rise to High Catalytic Activity. *J. Am. Chem. Soc.* **126**: 7452–7453.

Lyon LA, Meng Z, Singh N, Sorrell CD, St John A. 2009. Thermoresponsive microgel-based materials. *Chem. Soc. Rev.* **38**(4): 865–74.

Maddock SC, Pasetto P, Resmini M. 2004. Novel imprinted soluble microgels with hydrolytic catalytic activity. *Chem. Commun.* (5): 536–537.

Manesiotis P, Hall AJ, Emgenbroich M, Quaglia M, De Lorenzi E, Sellergren B. 2004.An enantioselective imprinted receptor for Z-glutamate exhibiting a binding induced color change. *Chem. Commun.* (20): 2278–2279.

Markowitz MA, Kust PR, Deng G, Schoen PE, Dordick JS, Clark DS, Gaber BP. 2000. Catalytic Silica Particles via Template-Directed Molecular Imprinting. *Langmuir* **16**: 1759–1765.

Mayes AG, Whitcombe MJ. 2005. Synthetic strategies for the generation of molecularly imprinted organic polymers. *Adv. Drug Deliv. Rev.* **57**: 1742–1778.

Meekel AP, Resmini M, Pandit UK. 1996. Regioselectivity and enantioselectivity in an antibody catalysed hetero Diels-Alder reaction. *Bioorg. Med. Chem.* **4**: 1051–1057.

Pasetto P, Flavin K, Resmini M. 2009. Simple spectroscopic method for titration of binding sites in molecularly imprinted nanogels with hydrolase activity. *Biosens. Bioelectron.* **25**: 572–578.

Pasetto P, Maddock SC, Resmini M. 2005. Synthesis and characterization of molecularly imprinted catalytic microgels for carbonate hydrolysis. *Anal. Chim. Acta* **542**: 66–75.

Resmini M, Gul S, Carter S, Sonkaria S, Topham CM, Gallacher G, Brocklehurst K. 2000. A general kinetic approach to investigation of active site availability in macromolecular catalysts. *Biochem. J.* **346**: 117–125.

Sellergren B, Allender CJ. 2005. Imprinted polymers: A bridge to advanced drug delivery. *Adv. Drug Del. Rev.* **57**: 1733–1741.

Sellergren B, Shea KJ. 1994. Enantioselective ester hydrolysis catalysed by imprinted polymers. *Tetrahedron: Asymmetry* **5**: 1403–1406.

Servant A, Haupt K, Resmini M. 2011. Tuning molecular recognition in water-soluble nanogels with enzyme-like activity for the Kemp elimination. *Chem. Eur. J.* **17**: 11052–11059.

Spegel P, Schweitz L, Nilsson S. 2003. Selectivity toward miltiple predeterminated targets in nanoparticle capillary electrochromatography. *Anal. Chem.* **75**: 6608–6613.

Spivak DA. 2005. Optimization, evaluation and characterization of molecuary imprinted polymers. *Adv. Drug Del. Rev.* **57**: 1779–1794.

Wilcox CS, Adrian JC, Webb TH, Zawacki FJ. 1992. Chemistry of synthetic receptors and functional group arrays. 18. Approaches to quantitative supramolecular chemistry. Hydrogen-bond-based molecular recognition phenomena and sigmoidal behavior in multicomponent mixtures. *J. Am. Chem. Soc.* **114**: 10189–10197.

Wulff G. 2002. Enzyme-like Catalysis by Molecularly Imprinted Polymers. *Chem. Rev.* **102**: 1–27.

Wulff G, Sarhan A. 1972. The use of polymers with enzyme-analogous structures for the resolution of racemates. *Angew. Chem. Int. Ed.* **11**: 341.

Wulff G, Vesper W, Grobeeinsler R, Sarhan A. 1977. Enzyme-analogue built polymers4. On the synthesis of polymers containing chiral cavities and their use for the resolution of racemate. *Makromolekulare Chemie-Macromol. Chem. Phys.* **178**: 2799–2816.

Ye L, Mosbachm K. 2001. Polymers Recognizing Biomolecules Based on a Combination of Molecular Imprinting and Proximity Scintillation: A New Sensor Concept. *J. Am. Chem. Soc.* **123**: 2901–2902.

Yilmaz E, Kucukyavuz Z. 1993. Monomer reactivity ratios of styrene-4-vinylpyridine copolymers at low and high conversions. *Polymer* **34**: 145–149.

Yoshimatsu K, Yamazaki T, Chronakis IS Yoshimatsu K, Yamazaki T, Chronakis IS, Ye L. 2011. *J. Appl. Polym. Sci.*. DOI: 10.1002/app.35150